Since January 2020 Elsevier has created a COVID-19 resource centre with free information in English and Mandarin on the novel coronavirus COVID-19. The COVID-19 resource centre is hosted on Elsevier Connect, the company's public news and information website.

Colloids and Surfaces B: Biointerfaces 182 (2019) 110341

Contents lists available at ScienceDirect

Colloids and Surfaces B: Biointerfaces

journal homepage: www.elsevier.com/locate/colsurfb

Label-free localized surface plasmon resonance biosensor composed of multi-functional DNA 3 way junction on hollow Au spike-like nanoparticles (HAuSN) for avian influenza virus detection

Taek Lee[a,*], Ga Hyeon Kim[a], Soo Min Kim[a], Keonyoung Hong[a], Younghun Kim[a], Chulhwan Park[a], Hiesang Sohn[a,**], Junhong Min[b,***]

[a] Department of Chemical Engineering, Kwangwoon University, Wolgye-dong, Nowon-gu, Seoul 01899, Republic of Korea
[b] School of Integrative Engineering Chung-Ang University, Heukseok-dong, Dongjak-gu, Seoul 06974, Republic of Korea

ARTICLE INFO

Keywords:
AI virus detection
HA protein
Multi-functional DNA
Localized surface plasmon resonance
Biosensor
Hollow Au spike-like nanoparticles

ABSTRACT

In the present study, we fabricated a label-free avian influenza (AIV H5N1) detection biosensor composed of a multi-functional DNA 3 way-Junction (3 W J) on a hollow Au spike-like nanoparticle (hAuSN) using a localized surface plasmon resonance (LSPR) method. To construct the multi-functional DNA (MF-DNA) as a bioprobe, the 3 W J was introduced. The proposed AIV detection bioprobe should contain three functionalities: target recognition, signal amplification, and connection to substrate. To achieve this goal, each piece of the DNA 3 W J was tailored to a hemagglutinin (HA) binding aptamer, FAM dye and thiol group, respectively. The assembly of each DNA 3 W J functional fragment was then confirmed by TBM-Native PAGE. Moreover, the hAuSN was immobilized on the indium-tin-oxide (ITO) substrate for LSPR measurement. The DNA 3 W J was immobilized onto the hAuSN electrode through the thiol-group of DNA 3 W J. The fabricated DNA 3 W J/hAuSN heterolayer on the ITO substrate was investigated by field emission scanning electron microscopy (FE-SEM) and atomic force microscopy (AFM). LSPR experiments were conducted to confirm HA protein binding to the DNA 3 W J/ hAuSN -modified electrode. The proposed biosensor can detected the HA protein in PBS buffer (LOD: 1 pM) as well as in the diluted chicken serum (LOD: 1 pM). The present study details a label-free, simple fabrication method consisted of DNA 3 W J/ hAuSN heterolayer that uses easy-to-tailor elements to detect not only AIV but also various viruses detection platform easily.

1. Introduction

With the increase in globalization as well as global warming, various new disease-causing viruses, such as dengue virus, zika virus, and MERS-CoV virus, have spread rapidly [1–3]. In particular, virus mutants are serious infectious pathogens because of their rapid infection speed, high infectivity and severe painful symptoms as well as the economic losses associated with their spread. Efforts to prevent such infections and develop vaccines against the viruses are underway [4]. The avian influenza virus (AIV) is particularly regarded as a highly contagious virus that infects humans and birds and, in the past, it has caused economic issues and health problems [5,6]. The highly pathogenic H5N1 AIV infection can be transferred from birds to humans and can cause death. Usually, bird flu can only infect bird species. However, AIV mutants (H5N1) can infect humans as well [7]. Furthermore, if a human is infected with H5N1 AIV, the virus can exchange genetic information with the human flu virus and then spread to other individuals.

To prevent the spread of H5N1 AIV, several techniques have been proposed to identify H5N1, including surface-enhanced Raman spectroscopy (SERS) [8], enzyme linked immunosorbent assay (ELISA) [9], electrochemical (EC) assays [10], quartz crystal microbalance (QCM) [11], Luminescence resonance energy transfer (LRET) [12], surface plasmon resonance (SPR) [13–15], and fluorescence [16] techniques. In order to create a portable H5N1 detection system for field use, it is important to meet the requirements of accuracy, high sensitivity, high throughput, specificity, fast signal response time, small sample size, and ease of use in the field. Among these, the optical biosensor-based

* Corresponding author at: Department of Chemical Engineering, Kwangwoon University, Republic of Korea.
** Corresponding author at: Department of Chemical Engineering, Kwangwoon University, Republic of Korea.
*** Corresponding author at: School of Integrative Engineering, Chung-Ang University, Republic of Korea.
E-mail addresses: tlee@kw.ac.kr (T. Lee), hsohn@kw.ac.kr (H. Sohn), junmin@cau.ac.kr (J. Min).

https://doi.org/10.1016/j.colsurfb.2019.06.070
Received 25 March 2019; Received in revised form 27 June 2019; Accepted 28 June 2019
Available online 02 July 2019
0927-7765/

localized surface plasmon resonance (LSPR) method has been studied for high sensitivity, easy fabrication, and cost-effectiveness [17,18]. Introduction of plasmonic nanostructures to virus detection could facilitate the field-ready portable biosensor construction. The electron oscillation originating from electromagnetic waves triggers a binding interaction event in the nanoparticle interface, thus providing high sensitivity [19]. Moreover, this plasmonic event can be tuned to excite the fluorescence dye-labeled bioprobe that exhibits ultra-sensitivity in order to detect the H5N1 virus [20,21]. Advanced bioprobes have been developed to detect H5N1 accurately with high sensitivity. Among these, DNA aptamers are one of the powerful elements used to construct an AIV biosensor [22,23]. However, to construct the aptasensor, a labeling process and immobilization process are usually required to enhance signals and fabricate the electrode. These processes are quite complicated, time-consuming, and laborious. Furthermore, conventional DNA only has two terminal groups at the 5′ and 3′, which limits embodying the multi-functionality and complicates the manufacture processes related to immobilization, labeling, and detection.

To overcome the present limitation, this study introduced the DNA 3-way junction (3 W J) that can introduce multi-functionality [24,25]. Compared to packaging RNA 3 W J (pRNA 3 W J), DNA 3 W J showed the less stability [26–28]. However, for the biosensor construction, the production cost issue should also be considered. DNA 3 W J is cheaper than same sequence of RNA 3 W J for constructing MF-DNA bioprobe. Each end of the DNA arm was modified to perform the biosensor function. The 5′ end of the DNA 3 W Ja was tagged to an HA protein recognition aptamer (HA Apt/3 W Ja). The 5′ end of DNA 3 W Jb was labeled with FAM dye (FAM/3 W Jb) for signal enhancement. It is reported that the fluorescence dye can be excited by a plasmonic field, which increases the detection sensitivity effectively [20,21]. To increase the LSPR enhancement effect, FAM dye was introduced. Moreover, the LSPR enhancement effect by fluorescence dye needs to adequate distance between fluorophore and nanoparticle surface [29,30]. The FAM-tagged DNA 3 W J showed the high rigidity and provide the defined distance around 5–6 nm between FAM and hAuSN surface for making LSPR effect. As the rest of module, the 5′ end of DNA 3 W Jc was labeled with a thiol-group (SH/3 W Jc) that enabled bioprobe immobilization without an additional linkage process. These functional DNA pieces were assembled well by annealing. The hAuSN-modified ITO substrate was also prepared by atmospheric plasma treatment and silanization. hAuSN has a unique local refractive index (RI) and high surface roughness that can provide increased bioprobe immobilization chances compared to normal Au nanoparticles [31]. This transparent substrate can provide a detection platform for LSPR. Synthesis of hAuSN was confirmed by field-emission scanning electron microscopy (FE-SEM). The immobilization process of the multi-functional DNA 3 W J on the hAuSN-modified ITO substrate was investigated by atomic force microscopy (AFM). The sensing performance of the proposed biosensor was investigated by UV-VIS, which showed the high sensitivity of longitudinal LSPR intensity to detect the HA protein. Fig. 1 displays the schematic diagram of the AIV biosensor.

2. Experimental details

2.1. Materials

The influenza A H5N1 (A/VietNam/1203/2004) Hemagglutinin/HA Protein (His & Fc Tag), Influenza A H1N1 (A/New Caledonia/20/99) Hemagglutinin / HA Protein (His Tag) and spike protein (S) were purchased from Sino Biology (China). For hAuSN synthesis, hydrogen tetrachloroaurate (III) hydrate was purchased from Kojima Chemicals Co. (Japan). Silver nitrate was purchased from Junsei (Japan). Hydrogen peroxide, Triton-X solution, ammonium sulfate, sodium hydroxide, (3-aminopropyl)triethoxysilane (APTES), cytochrome c (CYT C), bovine serum albumin (BSA), myoglobin (MYO) and chicken serum were purchased from Sigma-Aldrich (USA). The three fragments of DNA 3 W J were synthesized and purified using HPLC by Bioneer (South Korea). The sequence of the H5N1 HA aptamer-tagged 3 W Ja (HA Apt/3 W Ja) is 5′-GTG TGC ATG GAT AGC ACG TAA CGG TGT AGT AGA TAC GTG CGG GTA GGA AGA AAG GGA AAT AGT TGT CCT GTT GTT GCC ATG TGT ATG TGG G -3′; FAM/3 W Jb is FAM-5′−CCC ACA TAC TTT GTT GAT CC -3′; and SH/3 W Jc is SH-5′- GGA TCA ATC ATG GCA A -3′, respectively. All oligonucleotides were diluted in nuclease free water. These sequences were synthesized by Bioneer (South Korea). All chemicals were used as received.

2.2. Preparation of hAuSN

The hollow and spike-like gold nanoparticles (hAuSN) were synthesized by the galvanic replacement reaction (GRR) method between AgNPs and $HAuCl_4$ [31]. AgNPs as sacrificial materials were prepared as follows: First 10 mL of 0.025 M $AgNO_3$ was added to 80 mL of boiling water, followed by 1 wt% trisodium citrate dehydrate. The mixture was boiled for 20 min and cooled to room temperature. Then, hAuSN was prepared with the as-made AgNPs solution, as follows: 5 mL of AgNPs were dispersed in 25 mL of 3 mM HAuCl4, and 5 mL of 10 mM ascorbic acid was injected into the resulting solution. To enhance the dispersion stability in the aqueous phase during storage, 0.1 g/mL of PVP was added to the final solution at 50 °C for 6 h.

2.3. Fabrication of hAuSN on ITO substrate

hAuSN immobilization onto the ITO surface was performed as per previous reports [32]. ITO-coated glass substrates (10 Ω resistance, National Nanofab Center, South Korea) were cleaned by sonication for 30 min using 2% Triton X-100 solution, DIW, and ethanol, sequentially. After washing, to make the surface hydrophilic, ITO substrates were directed to atmospheric plasma for 5 min and 30 μL × 5% of APTES solution was dropped onto the ITO substrate for 1 h at room temperature for silanization. After washing the surface with ethanol, the APTES-modified ITO substrates were heated at 70 °C for 20 min to recover the organosilane molecules. Afterwards, 30 μL ×3000 ppm of hAuSN solution was dropped onto the APTES-modified ITO surface followed by incubation for 12 h at room temperature, to allow coupling with the amine group of APTES and the Au surface. Finally, the hAuSN-modified ITO electrode was rinsed with DI water and dried using a nitrogen stream to remove the unreacted hAuSN.

2.4. Assembly of multi-functional DNA 3WJ

DNA 3 W J fragments were labeled with a functional group to construct a multi-functional DNA structure. Sequence selection of the HA aptamer was performed as per a previous report [23]. HA aptamer was connected to 3 W Ja for the 3 W J assembly. For plasmonic signal enhancement, the FAM/3 W Jb was introduced. Finally, SH/3 W Jc was prepared for anchoring the hAuSN directly. The AIapt/FAM/SH-3 W J was assembled by annealing three corresponding DNA strands at an equimolar ratio in TMS buffer (40 mM Tris−HCl, 10 mM $MgCl_2$, 100 mM NaCl) by heating at 80 °C for 5 min, followed by slowly cooling down to 4 °C at a rate of 2 °C/min on a T100™ Thermal Cycler (Bio-rad). The assembled DNA biomarker was confirmed by 8% native TBM-PAGE (89 mM Tris, 200 mM boric acid, 5 mM $MgCl_2$, pH 7.6) [33].

2.5. Surface morphology analysis

The fabricated hAuSN-modified ITO substrates were investigated by FE-SEM (Auriga, Carl Zeiss, Germany). In addition, the biofilm fabrication was investigated by tapping-mode AFM (Digital Instruments, USA). The bare ITO substrate, hAuSN -modified ITO, DNA 3 W J self-assembled on hAuSN-modified ITO substrate, and HA protein/DNA 3 W J/ hAuSN-modified ITO substrate were investigated by AFM for comparison. Before scanning the sample, the set point current,

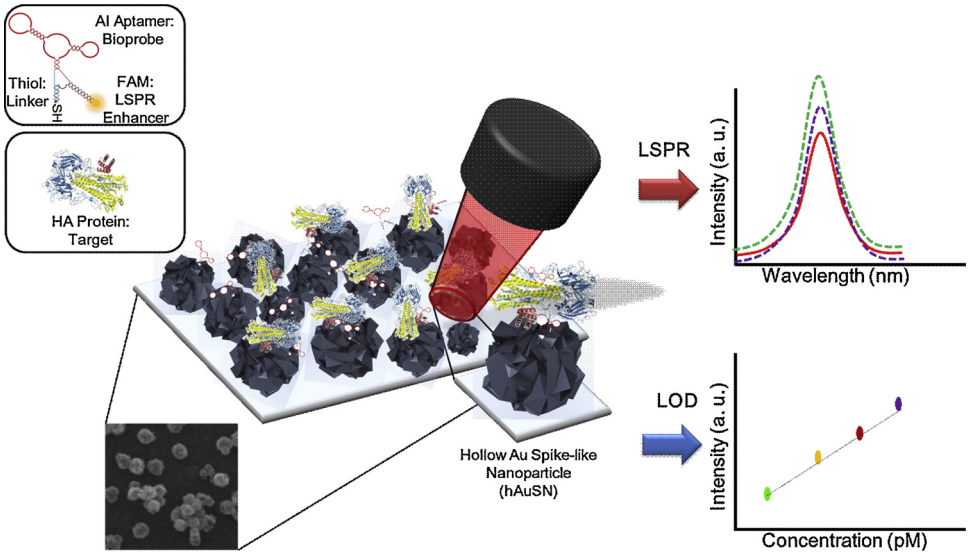

Fig. 1. Schematic image of the fabricated AIV detection biosensor based on LSPR method.

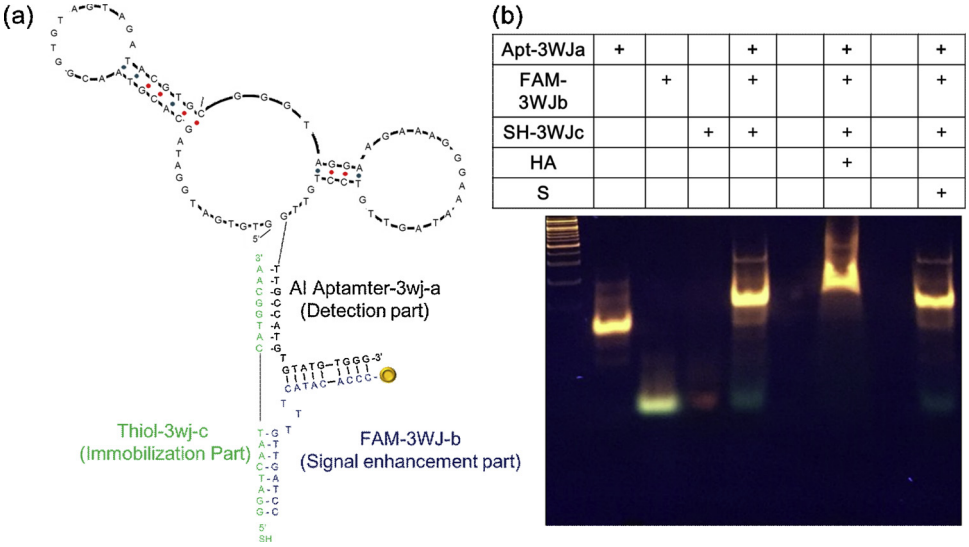

Apt-3WJa	+			+		+		+
FAM-3WJb		+		+		+		+
SH-3WJc			+	+		+		+
HA						+		
S								+

Fig. 2. (a) Schematic diagram of multi-functional DNA 3 W J for AIV H5N1 detection through LSPR, (b) TBM PAGE gel result of multi-functional DNA 3 W J, HA protein, spike protein.

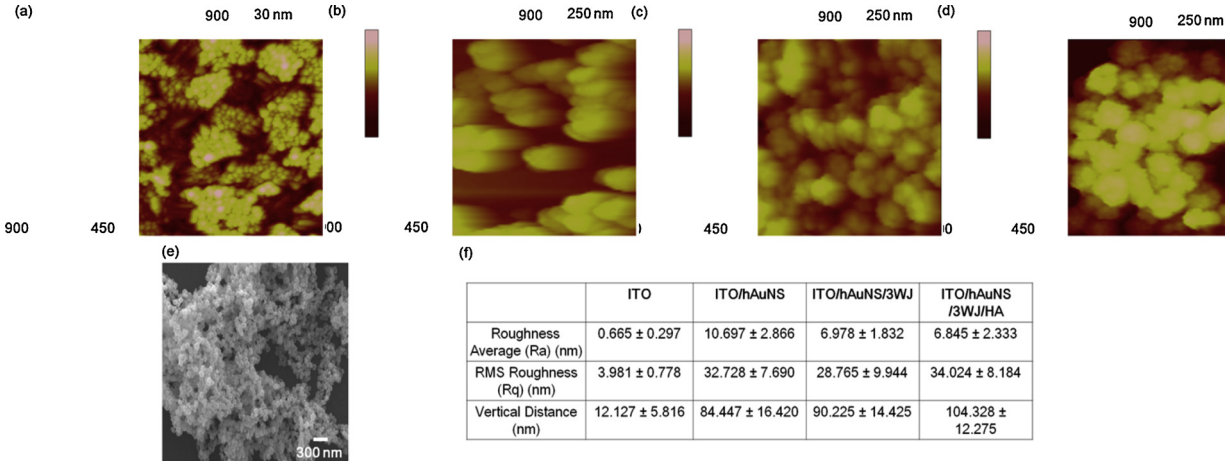

	ITO	ITO/hAuNS	ITO/hAuNS/3WJ	ITO/hAuNS /3WJ/HA
Roughness Average (Ra) (nm)	0.665 ± 0.297	10.697 ± 2.866	6.978 ± 1.832	6.845 ± 2.333
RMS Roughness (Rq) (nm)	3.981 ± 0.778	32.728 ± 7.690	28.765 ± 9.944	34.024 ± 8.184
Vertical Distance (nm)	12.127 ± 5.816	84.447 ± 16.420	90.225 ± 14.425	104.328 ± 12.275

Fig. 3. (a) Surface morphology of ITO substrate by AFM (b) hAuSN-immobilized on ITO substrate by AFM, (c) surface morphology of DNA 3 W J on hAuSN-immobilized ITO substrate by AFM, (d) Surface morphology of HA protein on DNA 3 W J /hAuSN/ITO by AFM, (e) Surface morphology of hAuSN-immobilized Au substrate by FE-SEM, (e) Surface roughness analysis of the ITO, hAuSN/ITO, DNA 3 W J /hAuSN/ITO and HA protein/ DNA 3 W J /hAuSN/ITO.

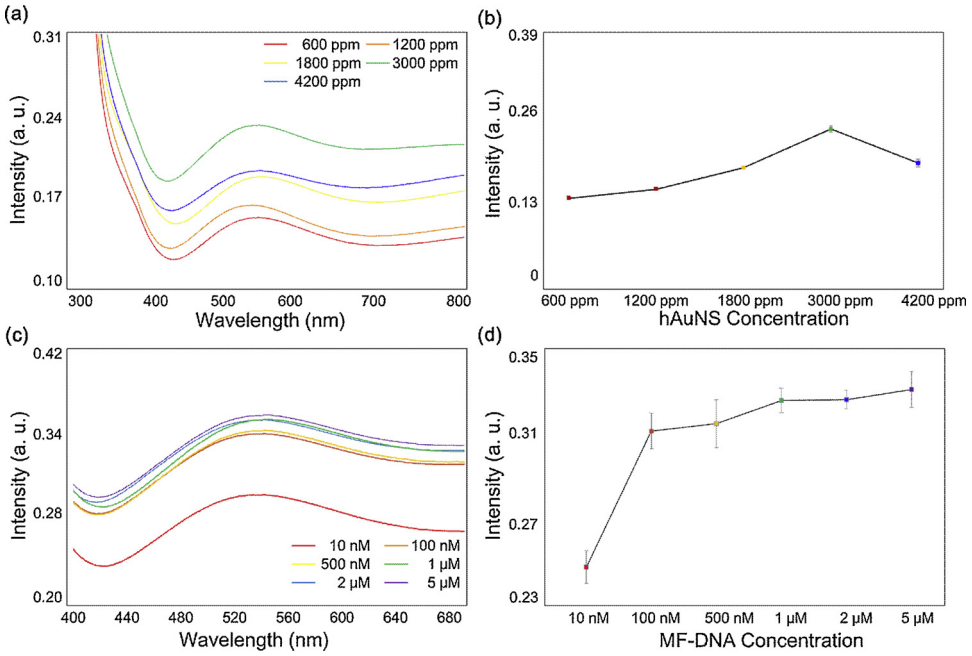

Fig. 4. Optimum conditions for HA protein detection using an aptamer-based localized surface plasmon resonance (LSPR) method. (a) Optical characteristics investigation on the effect of hAuSN concentrations on the ITO substrate (From 600 ppm to 4200 ppm). (b) The effect of hAuSN concentrations on the LSPR substrate. (c) Optical characteristics investigation on the effect of DNA 3 W J concentration on the LSPR substrate (From 10 nM to 5 μM). (d) The effect of DNA 3WJ concentration on the LSPR substrate. Error bar represents relative standard deviation of 5 independent experiments.

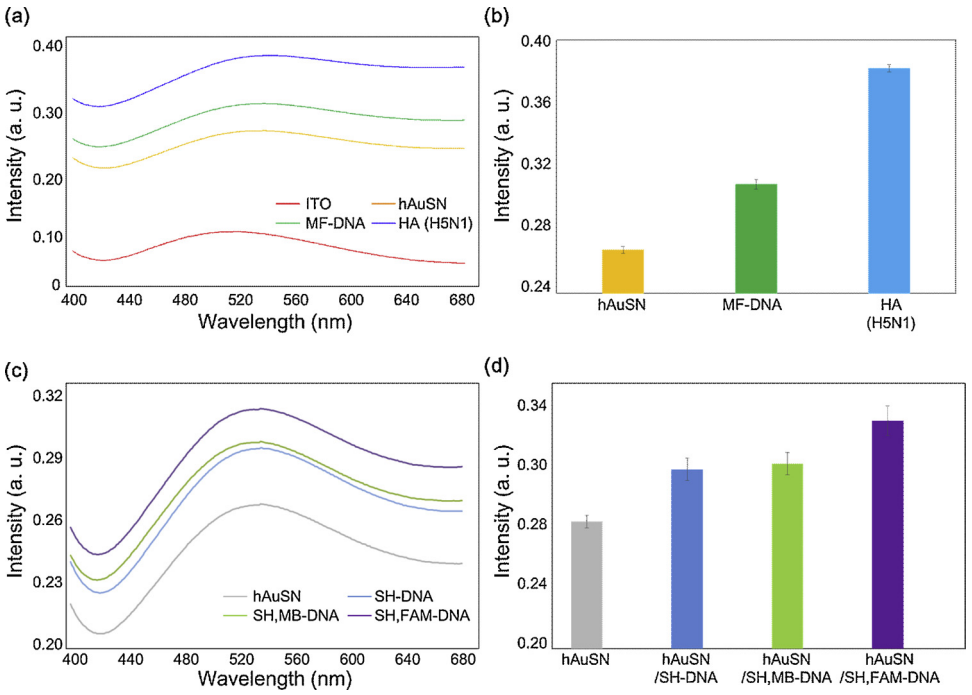

Fig. 5. (a) Optical characteristics of the bare ITO substrate (Red line), hAuSN on ITO substrate (Yellow line), DNA 3WJ immobilized layer on hAuSN/ITO (Green line), HA protein reacted with DNA 3WJ /hAuSN/ITO layer, respectively. (b) Change in absorbance peak based on immobilization about hAuSN, DNA 3WJ, HA protein layers, respectively. (c) Optical characteristics of hAuSN on ITO substrate (Grey line), SH-DNA immobilized layer on hAuSN/ITO (Blue line), SH,MB-DNA on hAuSN/ITO layer (Green line), SH,FAM-DNA (MF-DNA) on hAuSN/ITO layer (Purple line), respectively. (d) Change in absorbance peak based on immobilization of SH-DNA, SH,MB-DNA SH,FAM-DNA (MF-DNA), respectively. Error bar represents relative standard deviation of 10 independent experiments.

integrated gain and proportional gain were optimized to the force between the tip and the substrate surface [34].

2.6. Detection of HA protein by LSPR

To detect the AIV through the DNA 3 W J/ hAuSN substrate, ultraviolet-visible spectroscopy (UV-VIS) was used to measure the LSPR effect. Binding of HA protein to the AIapt/FAM/SH-DNA 3 W J was monitored by an LSPR absorbance intensity in the UV–vis spectrum resulting from changes in the local refractive index induced by the target-aptamer reaction. The local refractive index changes induced by target-aptamer interaction at a given wavelength are attributed to the extension of light absorption by the biofilm on the hAuSN-modified ITO electrode. All absorption spectra were obtained by monitoring UV–vis spectral changes in the transmission mode of JASCO V-530 UV-spectrometer (Japan) [18,19]. The measurement requires around 10 min.

3. Results and discussion

3.1. Confirmation of assembled multi-functional DNA 3WJ

For detecting the HA protein through LSPR methods, the multifunctional DNA 3 W J requires three functional groups: 1) HA protein recognition group, 2) immobilization group, and 3) LSPR signal enhancer. The HA protein aptamer was tagged to the 3 W Ja motif. FAM dye was tagged to the 3 W Jb motif, and the thiol-modified 3 W Jc was prepared. Each functional 3 W J fragment was assembled as AIapt/FAM/SH-DNA 3 W J (Fig. S1). Fig. 2a shows the expected AIapt/FAM/

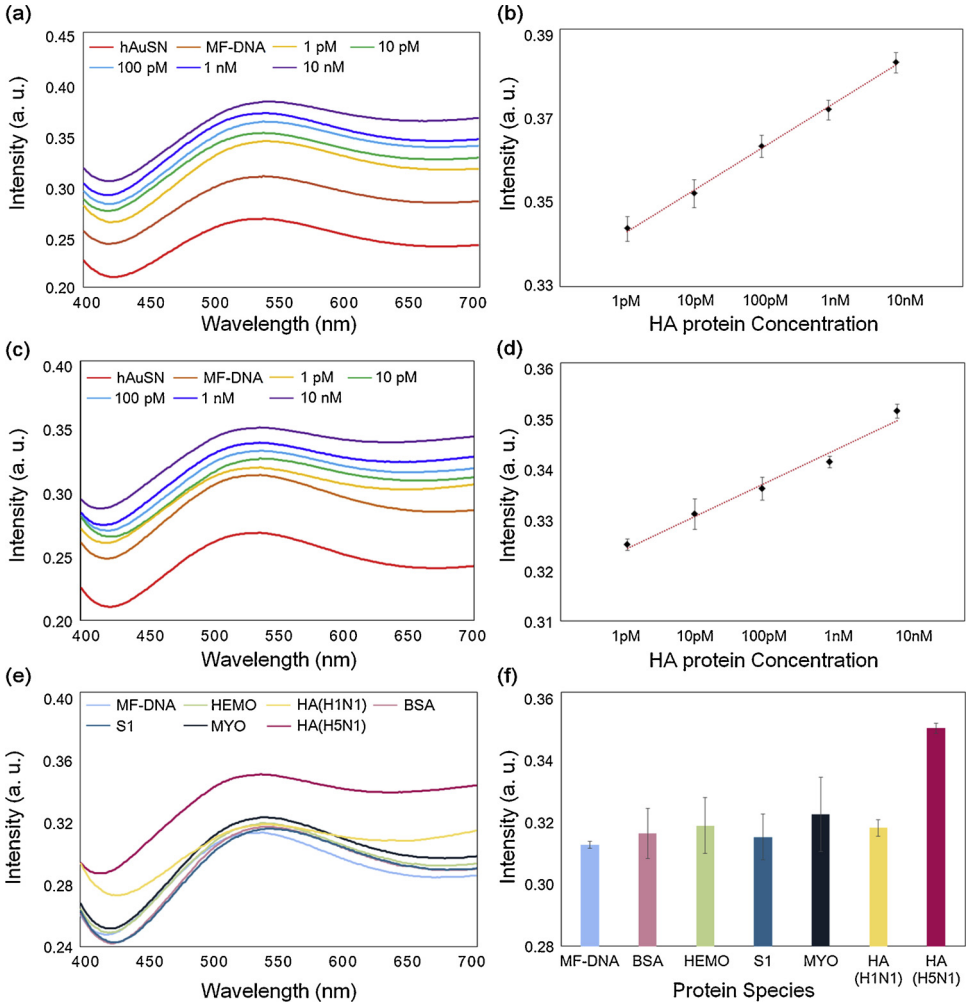

Fig. 6. (a) Detection of HA protein in PBS buffer on the MF-DNA/hAuSN-based localized surface plasmon resonance (LSPR) biosensor. Absorbance increases from different HA concentrations in PBS buffer (1 pM to 10 nM) of (b) Calibration characteristics of the different concentration of HA protein range from 1 pM to 10 nM with correlation coefficient (R^2) of 0.9976. (c) Detection of HA protein in 10% chicken serum on the DNA 3WJ -based localized surface plasmon resonance (LSPR) biosensor. Absorbance increases from different HA concentrations in 10% chicken serum (1 pM to 10 nM) of (d) Calibration characteristics of the different concentration of HA protein range from 1 pM to 10 nM with correlation coefficient (R^2) of 0.9796. (e) Selectivity test of DNA 3WJ/hAuSN-based LSPR biosensor with the various targets (cytochrome c (Blue line), BSA (Green line), spike protein (Grey line), myoglobin (Yellow line) and HA protein (Red line). (f) Change in absorbance peak based on selectivity test with other protein reaction (cytochrome c (Blue line), BSA (Green line), spike protein (Grey line), myoglobin (Yellow line) HA protein (H1N1) (Purple line) and HA protein (H5N1) (Red line), respectively. Error bar represents relative standard deviation of 15 independent experiments.

SH-DNA 3 W J 2D structure. Assembly of AIapt/FAM/SH-DNA 3 W J was confirmed by 8% native TBM-PAGE. Fig. 2b shows the PAGE result of the AIapt/Zyme/SH-DNA 3 W J assembly. The gel clearly shows the AIapt-3 W Ja (lane 2), FAM-3 W Jb (lane 3), SH-3 W Jc (lane 4), and AIapt/Zyme/SH-DNA 3 W J (lane 5). The results demonstrate that the designed multi-functional bioprobe can be prepared easily. However, the prepared multifunctional bioprobe should sustain its target binding affinity and specificity. HA protein was thus reacted with the assembled AIapt/FAM/SH-DNA 3 W J. Lane 7 shows the migration retard and upper band occurrence that clearly indicates the assembled AIapt/FAM/SH-DNA 3 W J-bound HA protein. As a negative control, the spike protein (S protein from MERS-CoV coat protein) was reacted with the assembled AIapt/FAM/SH-DNA 3 W J (lane 9). In case of lane 9, no migration change was observed compared to that in lane 5. This implies that the AIapt/FAM/SH-DNA 3 W J only showed specificity to HA protein. Therefore, the designed bioprobe can detect the HA protein specifically.

3.2. Investigation of fabricated HA protein/DNA 3WJ on the hAuSN heterolayer

The immobilization process of HA protein/DNA 3WJ on the hAuSN heterolayer on the ITO electrode was investigated by AFM and FE-SEM. Fig. 3(a) shows the AFM results of the ITO electrode surface. Small grains with sizes around 20–30 nm were observed on the ITO surface. After hAuSN immobilization via plasma treatment with the linker, numerous large hAuSN particles with high density were observed to be immobilized and the grain sizes are measured to be around 100–150 nm. The AFM result of the hAuSN-modified surface clearly exhibited the nanoparticle morphology (Fig. 3b). Fig. 3c exhibited the DNA 3 W J immobilized on the hAuSN ITO electrode. It formed small lumps with sizes around 30–40 nm on the hAuSN particles, so it might be assumed that the DNA 3 W J was immobilized on the hAuSN particles. After the HA protein reacted with the immobilized bioprobe-modified surface, the AFM morphology was changed with a vertical height size increment compared to the DNA 3 W J molecule using horizontal analysis (Fig. 3d). Fig. 3(e) shows the FE-SEM image analysis with a large area clearly showing the hAuSN immobilized on the ITO surface (Fig. S2, Fig. S3). The vertical size of the HA protein that we obtained was around 14 nm through vertical analysis (Fig. 3f). The surface roughness analysis was also performed (Fig. 3f). The combined results indicate that the fabricated heterolayer immobilized well on the ITO substrate.

3.3. Optimization test of DNA 3 W J/ hAuSN heterolayer fabrication

When hAuSN was immobilized onto the ITO substrate, the LSPR band was observed in the visible range. This result shows that the hAuSN layer substrate could be applied to the LSPR biosensor for HA detection. To maximize the LSPR effect of hAuSN, various concentrations of hAuSN were employed on the ITO substrate and changes in absorbance were monitored to obtain the optimal concentration of hAuSN for LSPR biosensor fabrication. Fig. 4a shows the UV-VIS absorption spectra with various concentrations (600 ppm, 1200 ppm, 1800 ppm, 3000 ppm, and 4200 ppm) of the hAuSN layer. Because of free electron absorption, the hAuSN layer absorbed light throughout the

Table 1
Comparison of the proposed biosensor with other biosensors for AIV detection in terms of materials, detection method, sensitivity (LOD) and labeling step.

No.	Materials	Detection Method	Detection Limit	Label-free or not	References
1	Aptamer / Ag@SiO_2 nanoparticle	Fluorescence	2 ng/ml (in aqueous buffer) 3.5 ng/ml (in Human serum)	Label-free	[16]
2	Aptamer / Gold nanoparticle	EIS	0.125 HAU (pure virus) 1 HAU (tracheal chicken swab samples spiked with the H5N1 virus)	Gold Nanoparticle	[10]
3	Oligonucleotide	Luminescence Resonance Energy Transfer	7 pM	Upconversion nanoparticles	[12]
4	RNA	Surface-enhanced Raman scattering (SERS)	2.67 aM	Raman	[8]
5	Aptamer / Stereptavidin-biotin	SPR	0.128 HAU	Label-free	[13]
6	Oligonucleotide/ Gold nanoarray	LSPR	$2.36 \times 10^{13}/cm^2$ oligonucleotides	Gene	[14]
7	Aptamer-Cojugated Gold nanoparticle	SPR	200 EID_{50}/ml	Virus	[15]
8	Recombinant Antibody	IM-SPR	144 copies/mL	HA	[35]
9	MF-DNA/hAuSN	LSPR	1 pM	Label-free	Present work

visible ranges and an absorption peak was observed at around 541 nm. When the hAuSN concentration was changed, the LSPR peak intensity was changed. From 600 ppm (red line) to 3000 ppm (green line), the LSPR peak intensity was gradually increased. However, at 4200 ppm of hAuSN-modified ITO the LSPR peak intensity was decreased (Fig. 4b). This effect might be elucidated by hampered light transmission due to physical adsorption and unreacted particles of hAuSN. Based on these results, we employed 3000 ppm of hAuSN for LSPR biosensor fabrication.

Moreover, various concentrations of bioprobes were immobilized on the hAuSN-modified ITO substrate to obtain optimal conditions. Fig. 4c depicts the UV-VIS absorption spectra of various concentrations (10 nM, 100 nM, 500 nM, 1 μM, 2 μM, and 5 μM) of DNA 3 W J layers immobilized on the hAuSN-modified substrate. From 10 nM (red line) to 1 μM (green line), the LSPR peak intensity was gradually increased. However, with 2 μM of DNA 3 W J immobilization (blue line), the LSPR peak intensity (Fig. 4d) was slightly decreased compared to that with 1 μM of DNA 3 W J. This effect might be elucidated by hampered light transmission due to the physical adsorption of DNA 3 W J. In case of the 5 μM of DNA 3 W J immobilization (purple line), the LSPR intensity was slightly increased compared to that with 1 μM of DNA 3 W J. However, for cost-effectiveness, 1 μM of DNA 3 W J is suitable for further experiments.

3.4. Plasmon effect characterization of HA protein/ DNA 3WJ on hAuSN

To confirm the LSPR effect, a UV-VIS experiment was carried out using the hAuSN -modified ITO substrate. The yellow curve in Fig. 5a shows the LSPR peak at around 541 nm. Compared with UV-VIS spectra of the ITO substrate (red line), the hAuSN layer absorbed light from the visible area because of free electron absorption [19]. After DNA 3 W J immobilization, the LSPR band intensity was increased substantially (green line). Then, when HA protein was added to the DNA 3 W J/ hAuSN -modified substrate, an additional increase in the LSPR band was observed (blue line). This phenomenon could be explained by the increased thickness of the protein-DNA biomolecular layers on the hAuSN nanostructure through the plasmon effect. This also indicated that the prepared bioprobe (DNA 3 W J) reacted well with the target HA protein.

Moreover, to increase the LSPR effect on the fabricated DNA 3 W J/ hAuSN substrate, we compared the three types of DNA 3 W J. Fig. 5b shows the absorbance peaks of SH-modified DNA 3 W J (yellow line), MB/SH-modified DNA 3 W J (green line), and FAM/SH-modified DNA 3 W J (cobalt line), respectively. Comparison with SH-DNA 3 W J and MB/SH-DNA 3 W J, little absorbance change was observed. However, in the case of FAM/SH-DNA 3 W J, a substantially increased LSPR band was observed compared to that with SH-DNA 3 W J. Presumably, the results showed that the fluorescent dye molecule in the DNA could couple with the surface plasmon that confers a high refractive index onto the DNA 3 W J-modified hAuSN substrate [21]. Based on the combined result, the prepared nanobio heterolayer can be used to effectively detect HA protein.

3.5. Detection performance and clinical test

To analyze the LSPR biosensor performance considering the LOD and dynamic range, LSPR experiments were carried out with 9 samples. The HA protein diluted in PBS buffer was added to the DNA 3 W J/ hAuSN-modified biosensor for 3 h at RT. After the washing step, the LOD was measured. The LSPR band was obtained corresponding to the HA protein concentration (0 pM to 100 nM). To analyze the detection performance and limit of detection (LOD), various concentrations of serially diluted HA protein in PBS buffer were used. As shown in Fig. 6a, the LSPR peak intensity increased with increasing HA protein concentration between 1 pM to 100 nM. This clearly showed a linear relationship between LSPR intensity and HA protein concentration in this

range with an R^2 of 0.9976 (Fig. 6b).

Based on a successful linear relationship between the target concentration and LSPR band intensity, the fabricated biosensor was tested with HA protein in 10-fold diluted chicken serum for clinical testing (Fig. 6c). Compared to HA protein diluted in PBS buffer, the LSPR band intensity and peak wavelength was somewhat volatile. This might be explained by the unreacted proteins in chicken serum residues physically binding to the fabricated DNA 3 W J/ hAuSN-modified heterolayer. Fig. 6d exhibited a linear relationship between various concentrations of the HA protein and LSPR intensity. Compared with 6b, this curve showed low R^2 at 0.9796. Nevertheless, the fabricated LSPR biosensor can clearly detect HA protein within 10 min.

In addition, the selectivity of fabricated LSPR biosensor was tested with other proteins including cytochrome c (CYT C), bovine serum albumin (BSA), spike protein (S), myoglobin (MYO) and HA protein (H1N1) in the diluted chicken serum as negative controls (Fig. 6e). The result showed little LSPR intensity increase compared to that when the HA protein was added to the fabricated MF-DNA/hAuSN-modified heterolayer (Fig. 6f). The performance comparison of the fabricated LSPR biosensor performance comparison between the present HA detection biosensor and other biosensors reported is summarized in Table 1 [29]. Thus, the proposed LSPR biosensor can successfully detected the HA protein in clinical samples with high selectivity.

4. Conclusions

Avian influenza virus is one of the most serious virus pathogens in birds and humans due to rapid infection, various mutants, and dangerous symptoms. In this study, the authors developed an LSPR biosensor composed of DNA 3 W J on a hAuSN -modified ITO electrode. The MF-DNA was introduced as a multi-functional bioprobe for simultaneous HA protein detection, LSPR signal enhancement, and immobilization. Construction of the multi-functional DNA was confirmed by TBM-PAGE. The hAuSN-modified ITO substrate can be easily prepared and provides a suitable detection platform for LSPR methods. AFM and FE-SEM experiments were carried out to investigate the surface topography of the hAuSN-modified ITO substrate. Moreover, LSPR measurements were then carried out to determine HA protein binding to DNA 3 W J on the hAuSN-modified electrode. For the clinical test, specificity tests and LOD tests were carried out. Respective LSPR-based AIV detection platforms have been developed. However, the proposed method can perform each experiment on a single platform without an additional labeling, immobilization, and target amplification processes. In the near future, this simple H5N1 biosensor fabrication method can be used as a powerful alternative for virus detection platforms.

Acknowledgments

This research was supported by Basic Science Research Program through the National Research Foundation of Korea (NRF) funded by the Ministry of Education (2018R1D1A1B07049407), and by BioNano Health-Guard Research Center funded by the < GS3 > Ministry of Science and ICT < GS3 > (MSIT) of Korea as a Global Frontier Project (Grant number H-GUARD_2018M3A6B2057261).

Appendix A. Supplementary data

Supplementary material related to this article can be found, in the online version, at doi:https://doi.org/10.1016/j.colsurfb.2019.06.070.

References

[1] I.A. Rodenhuis-Zybert, J. Wilschut, J.M. Smit, Dengue virus life cycle: viral and host factors modulating infectivity, Cell. Mol. Life Sci. 67 (2010) 2773–2786.
[2] R.W. Malone, J. Homan, M.V. Callahan, J. Glasspool-Malone, L. Damodaran, A.D. Schneider, R. Zimler, J. Talton, R.R. Cobb, I. Ruzic, J. Smith-Gagen, D. Janies, J. Wilson, Zika virus: medical countermeasure development challenges, PLoS Negl. Trop. Dis. 10 (2016) e0004530.
[3] A. Zumla, D.S. Hui, S. Perlman, Middle east respiratory syndrome, Lancet 386 (2015) 995–1007.
[4] V. Sikka, V.K. Chattu, R.K. Popli, S.C. Galwankar, D. Kelkar, S.G. Sawicki, S.P. Stawicki, T.J. Papadimos, The emergence of Zika virus as a global health security threat: a review and a consensus statement of the INDUSEM Joint Working Group (JWG), J. Global Infect. Dis. 8 (2016) 3.
[5] D.J. Alexander, I.H. Brown, History of highly pathogenic avian influenza, Rev. Sci. Tech. 28 (2009) 19–38.
[6] T. Lee, J.H. Ahn, S.Y. Park, G.H. Kim, J. Kim, T.H. Kim, I. Nam, C. Park, M.H. Lee, Recent advances in AIV biosensors composed of nanobio hybrid material, Micromachines 9 (2018) 651.
[7] E. Basuno, Y. Yusdja, Ilham N, Socio-economic impacts of avian influenza outbreaks on small-scale producers in Indonesia, Trans Emerg. Dis. 57 (2010) 7–10.
[8] Y. Pang, J. Wang, R. Xiao, S. Wang, SERS molecular sentinel for the RNA genetic marker of PB1-F2 protein in highly pathogenic avian influenza (HPAI) virus, Biosens. Bioelectron. 61 (2014) 460–465.
[9] I. Shiratori, J. Akitomi, D.A. Boltz, K. Horii, M. Furuichi, I. Waga, Selection of DNA aptamers that bind to influenza A viruses with high affinity and broad subtype specificity, Biochem. Biophys. Res. Commun. 443 (2014) 37–41.
[10] S. Karash, R. Wang, L. Kelso, H. Lu, T.J. Huang, Y. Li, Rapid detection of avian influenza virus H5N1 in chicken tracheal samples using an impedance aptasensor with gold nanoparticles for signal amplification, J. virological methods. 236 (2016) 147–156.
[11] D. Li, J. Wang, R. Wang, Y. Li, D. Abi-Ghanem, L. Berghman, B. Hargis, H. Lu, A nanobeads amplified QCM immunosensor for the detection of avian influenza virus H5N1, Biosens. Bioelectron. 26 (2011) 4146–4154.
[12] W.W. Ye, M.K. Tsang, X. Liu, M. Yang, J. Hao, Upconversion luminescence resonance energy transfer (LRET)-based biosensor for rapid and ultrasensitive detection of avian influenza virus H7 subtype, Small 10 (2014) 2390–2397.
[13] H. Bai, R. Wang, B. Hargis, H. Lu, Y. Li, A SPR aptasensor for detection of avian influenza virus H5N1, Sens. 12 (2012) 12506–12518.
[14] S.A. Kim, K.M. Byun, K. Kim, S.M. Jang, K. Ma, Y. Oh, D. Kim, S.G. Kim, M.L. Shuler, S.J. Kim, Surface-enhanced localized surface plasmon resonance biosensing of avian influenza DNA hybridization using subwavelength metallic nanoarrays, Nanotechnology 21 (2010) 355503.
[15] V.T. Nguyen, H.B. Seo, B.C. Kim, S.K. Kim, C.S. Song, M.B. Gu, Highly sensitive sandwich-type SPR based detection of whole H5Nx viruses using a pair of aptamers, Biosens. Bioelectron. 86 (2016) 293–300.
[16] Y. Pang, Z. Rong, J. Wang, R. Xian, S. Wang, A fluorescent aptasensor for H5N1 influenza virus detection based-on the core–shell nanoparticles metal-enhanced fluorescence (MEF), Biosens. Bioelectron. 66 (2015) 527–532.
[17] S. Unser, I. Bruzas, J. He, L. Sagle, Localized surface plasmon resonance biosensing: current challenges and approaches, Sensors 15 (2015) 15684–15716.
[18] S.Y. Oh, N.S. Heo, S. Shukla, H.J. Cho, A.T. Ezhilvilian, J. Kim, S.Y. Lee, Y.K. Han, S.M. Yoo, Y.S. Huh, Development of gold nanoparticle-aptamer-based LSPR sensing chips for the rapid detection of Salmonella typhimurium in pork meat, Sci. Rep. 7 (2017) 10130.
[19] J.H. Lee, B.C. Kim, B.K. Oh, J.W. Choi, Highly sensitive localized surface plasmon resonance immunosensor for label-free detection of HIV-1, Nanomed. Nanotechnol. Biol. Med. 9 (2013) 1018–1026.
[20] N.H.T. Tran, K.T.L. Trinh, J.H. Lee, W.J. Yoon, H. Ju, Reproducible enhancement of fluorescence by bimetal mediated surface plasmon coupled emission for highly sensitive quantitative diagnosis of double-stranded DNA, Small 14 (2018) 1801385.
[21] N.H.T. Tran, K.T.L. Trinh, J.H. Lee, W.J. Yoon, H. Ju, Fluorescence enhancement using bimetal surface plasmon-coupled emission from 5-carboxyfluorescein (FAM), Micromachines 9 (2018) 460.
[22] L. Xu, R. Wang, L.C. Kelso, Y. Ying, Y. Li, A target-responsive and size-dependent hydrogel aptasensor embedded with QD fluorescent reporters for rapid detection of avian influenza virus H5N1, Sens. Actuators B Chem. 234 (2016) 98–108.
[23] I. Shiratori, J. Akitomi, D.A. Boltz, K. Horii, M. Furuichi, I. Waga, Selection of DNA aptamers that bind to influenza A viruses with high affinity and broad subtype specificity, Biochem. Biophys. Res. Commun. 443 (2014) 37–41.
[24] Y. Xia, S. Gan, Q. Xu, X. Qiu, P. Gao, S. Huang, A three-way junction aptasensor for lysozyme detection, Biosens. Bioelectron. 39 (2013) 250–254.
[25] T. Lee, S.Y. Park, H. Jang, G.H. Kim, Y. Lee, C. Park, M. Mohammadniaei, M.H. Lee, J. Min, Fabrication of electrochemical biosensor consisted of multi-functional DNA structure/porous au nanoparticle for avian influenza virus (H5N1) in chicken serum, Mater. Sci. Eng. C 99 (2019) 511–519.
[26] X. Piao, H. Wang, D.W. Binzel, P. Guo, Assessment and comparison of thermal stability of phosphorothioate-DNA, DNA, RNA, 2′-F RNA, and LNA in the context of Phi29 pRNA 3WJ, RNA 24 (2018) 67–76.
[27] D. Shu, Y. Shu, F. Haque, S. Abdelmawla, P. Guo, Thermodynamically stable RNA three-way junctions for constructing multifuntional nanoparticles for delivery of therapeutics, Nat. Nanotechnol. 6 (2011) 658–667.
[28] Y. Shu, D. Shu, F. Haque, P. Guo, Fabrication of pRNA nanoparticles to deliver therapeutic RNAs and bioactive compounds into tumor cells, Nat. Protoc. 8 (2013) 1635–1659.
[29] M. Chekini, R. Filter, J. Bierwagen, A. Cunningham, C. Rockstuhl, T. Burgi, Fluorescence enhancement in large-scale self-assembled gold nanoparticle double arrays, J. Appl. Phys. 118 (2015) 233107.
[30] K.A. Kang, J. Wang, J.B. Jasinski, S. Achilefu, Fluorescence manipulation by gold nanoparticles: from complete quenching to extensive enhancement, Int. J. Nanobiotechnology Pharm. 9 (2011) 16.
[31] S. Han, K. Hang, J. Hong, D.Y. Yoon, C. Park, Y. Kim, Photothermal cellulose-patch

with gold-spiked silica microrods based on Escherichia coli, ACS Omega 3 (2018) 5244–5251.
[32] M. Mohammadniaei, J. Yoon, T. Lee, J.W. Choi, Spectroelectrochemical detection of microRNA-155 based on functional RNA immobilization onto ITO/GNP nanopattern, J. Biotechnol. 274 (2018) 40–46.
[33] T. Lee, Y. Lee, S.Y. Park, K. Hong, Y. Kim, C. Park, Y.-H. Chung, M.-H. Lee, J. Min, Fabrication of electrochemical biosensor composed of multi-functional DNA structure/Au nanospike on micro-gap/PCB system for detecting troponin I in human serum, Colloids Surf. B Biointerfaces 175 (2019) 343–350.
[34] T. Lee, S.U. Kim, J. Min, J.W. Choi, Multilevel biomemory device consisting of recombinant azurin/cytochrome c, Adv. Mater. 22 (2010) 510–514.
[35] Y.F. Chang, W.H. Wang, Y.W. Hong, R.Y. Yuan, K.H. Chen, Y.W. Huang, P.L. Lu, Y.H. Chen, Y.M.A. Chen, L.C. Su, S.F. Wang, Simple strategy for rapid and sensitive detection of avian influenza A H7N9 virus based on intensity-modulated SPR biosensor and new generated antibody, Anal. Chem. 90 (2018) 1861–1869.